

Chemically activated sugarcane bagasse for biosorption of ibuprofen from aqueous solution

Bagaço de cana-de-açúcar ativado quimicamente para a bio sorção de ibuprofeno de solução aquosa

Bruna Assis Paim dos Santos¹, Evandro Luiz Dall'Oglio², Adriano Buzutti de Siqueira², Leonardo Gomes de Vasconcelos², Eduardo Beraldo de Moraes^{1,3}

¹Programa de Pós-Graduação em Recursos Hídricos, Universidade Federal de Mato Grosso, (PPGRH/UFMT), Av. Fernando Corrêa da Costa, 2367, CEP: 78060-900, Cuiabá, MT, Brasil.

²Departamento de Química, Universidade Federal de Mato Grosso (DQ/UFMT), Av. Fernando Corrêa da Costa, 2367, CEP: 78060-900, Cuiabá, MT, Brasil.

³Departamento de Engenharia Sanitária e Ambiental, Universidade Federal de Mato Grosso, (DESA/UFMT), Av. Fernando Corrêa da Costa, 2367, CEP: 78060-900, Cuiabá, MT, Brasil.

e-mail: bruna.santos_assis@hotmail.com; dallochio.evandro@gmail.com; buzutti7@hotmail.com; vasconceloslg@gmail.com; beraldo_morais@yahoo.com.br

ABSTRACT

In this study, the ability of chemically activated sugarcane bagasse (CASB) as a biosorbent for removing ibuprofen (IBP) from aqueous solution was evaluated. Sugarcane bagasse was activated using hexane and methanol. The effects of pH, contact time, IBP concentration, and temperature were evaluated in batch studies. Higher removal rates of IBP were found at pH 2.0. Kinetic studies indicated that the biosorption follows the pseudo-second-order model. The equilibrium biosorption isotherm was found to follow both Langmuir and Freundlich isotherm models. The maximum biosorption capacity of CASB was estimated at 7.75 mg g⁻¹ at 20 °C. According to the Dubinin-Radushkevich isotherm model, the activation energy was calculated to be 7.07 kJ mol⁻¹, indicating that a physical process mediated the IBP removal. Thermodynamic analysis suggests that the biosorption is exothermic in nature and non-spontaneous. The FTIR analysis confirmed the interactions between IBP molecules and biosorbent. We concluded that CASB exhibited the potential to be used in the removal of IBP from aqueous media.

Keywords: Ibuprofen removal, Kinetic, Isotherms, Thermodynamic study, Pharmaceutical drugs

RESUMO

Neste estudo, avaliou-se o bagaço de cana-de-açúcar quimicamente ativado (CASB) como bio sorvente na remoção de ibuprofeno (IBP) de solução aquosa. O bagaço da cana-de-açúcar foi ativado com hexano e metanol. Os efeitos do pH, tempo de contato, concentração de IBP e temperatura foram avaliados em estudos de bateladas. As taxas mais altas de remoção de IBP foram encontradas em pH 2,0. Estudos cinéticos indicaram que a bio sorção segue o modelo de pseudo-segunda ordem. Os dados no equilíbrio se ajustaram aos modelos de isoterma de bio sorção de Langmuir e Freundlich. A capacidade máxima de bio sorção do CASB foi estimada em 7,75 mg g⁻¹ a 20 °C. De acordo com o modelo de isoterma de Dubinin-Radushkevich, a energia de ativação foi calculada em 7,07 kJ mol⁻¹, indicando que o processo de remoção do IBP é físico. A análise termodinâmica sugere que a bio sorção é de natureza exotérmica e não espontânea. A análise de FTIR confirmou as interações entre as moléculas de IBP e o bio sorvente. Concluímos que o CASB exibiu potencial para ser utilizado na remoção do IBP de meio aquoso.

Palavras-chave: Remoção de ibuprofeno, Cinética, Isotermas, Estudo termodinâmico, Medicamentos

1. INTRODUCTION

In recent years, pharmaceutical compounds (PhCs) have been detected in sewage effluents [1], surface and ground waters [2], sediments [3], reservoir waters [4], and even in drinking waters [5]. This situation has

become a worldwide concern because many PhCs are persistent, bioaccumulative, and endocrine disruptors [6]. The untreated or inappropriately treated sewage is the primary cause of PhCs in the water bodies [7]. Thus, it is an emerging need to develop technologies to remove these compounds from aquatic media.

Ibuprofen (IBP) is a non-steroidal anti-inflammatory drug usually prescribed to relieve aches, pains, and fever. It has been detected in effluents from wastewater treatment plants in concentrations up to 22 µg/L [8] and in drinking water in concentrations up to 223.6 ng/L [9]. These concentrations are potentially hazardous to human health and ecosystems. Genotoxic effects of IBP at 300 ng/L was observed to the *Oreochromis niloticus* fish (Tilapia) [10]. The products of IBP degradation are also harmful. 4-isobutylacetophenone is formed by several pathways during its degradation and is toxic to red blood cells, connective tissue cells, and the central nervous system [11].

Various techniques have been employed to remove IBP from aqueous media such as electrochemical degradation [12], heterogeneous-Fenton process [13], photocatalytic degradation using TiO₂/UV [14], ultrasonic degradation [15], ozonation [16], and constructed wetlands [17]. However, the high cost of equipment, intensive energy requirements, the formation of toxic by-products, and the need for skilled personnel are some drawbacks and limitations that make these technologies impractical and expensive to operate. On the other hand, adsorption technology is an efficient and economical alternative to remove several pollutants from water and wastewater [18]. This technology has been applied for removing dyes, pesticides, heavy metals, and PhCs, including ibuprofen [19-23].

Recently, agricultural wastes have been extensively studied for adsorption of PhCs. These wastes include bean husk [24], onion skin [25], corncob [26], *Luffa cylindrica* [27], orange bagasse [28], and cocoa shell [29]. To improve the removal of PhCs, different chemical agents have been used to modify the functional groups on the biosorbent surface. Mondal et al. have prepared a N-modified *Parthenium hysterophorus* derived biochar to increase IBP removal [30]. Abbas et al. have improved the biosorption capacity of onion skin for IBP after treatment with HCl, H₂SO₄, and H₃PO₄ [31]. Chakraborty et al. have increased the removal of IBP using a sugarcane bagasse biochar activated by H₃PO₄ [32].

Bagasse is the waste obtained after sugarcane is milled for juice extraction. Sugarcane bagasse consists roughly of cellulose (40-45 %), hemicellulose (30-35 %), and lignin (20-30 %) [33]. As a by-product of sugar and renewable energy industries, sugarcane bagasse is an exciting material for developing biosorbent materials. Therefore, this study investigated the biosorption of IBP by chemically activated sugarcane bagasse under different experimental conditions of pH, contact time, temperature, and IBP concentration. Equilibrium isotherm, biosorption kinetics, and thermodynamic parameters were also analyzed, and IBP removal mechanisms were explored by Fourier transform infrared spectroscopy (FTIR).

2. MATERIALS AND METHODS

2.1 Chemicals

Ibuprofen sodium salt (IBP) (CAS no. 31121-93-4, molecular weight: 228.26 g mol⁻¹) was purchased from Sigma Aldrich (>98% purity, pK_a = 4.91). The molecular structure of IBP is represented in Fig. 1. Hexane, methanol, HCl, and NaOH were of analytical grade.

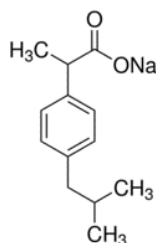


Figure 1: Chemical structure of IBP.

2.2 Preparation of biosorbent

Sugarcane bagasse (SB) was provided by Barralcool sugar and alcohol mill, Mato Grosso, Brazil, as waste biomass. SB was cut in small pieces, washed with abundant distilled water to remove dirt and traces of sugar, and dried in an oven at 80 °C for 24 h. After that, dry SB was ground to a fine powder using a steel-knife electrical mill and sieved through a 149 µm standard sieve. The SB was defatted by extraction with hexane for 6 h and posteriorly with methanol for another 6 h. The extraction occurred in a Soxhlet extractor. Follow-

ing the process, the chemically activated sugarcane bagasse by hexane and methanol (CASB) was rinsed with distilled water and dried in an oven at 80 °C for 24 h. The CASB was kept in a desiccator until use.

2.3 Biosorbent analysis

The point of zero charge (pH_{PZC}) of CASB was determined using the method described by Dahri *et al.* [34]. The experiment was performed in a series of 100 mL Erlenmeyer flasks filled with 25 mL of KNO_3 solutions (0.1 M) and 0.20 g of CASB. Aqueous solutions of 0.1 M of NaOH and 0.1 M of HCl were used for adjustment of pH of the KNO_3 solutions to the pH range of 2.5–10.0. Finally, the KNO_3 solutions were agitated for 24 h, at 23 °C, and the final pH was measured. The determination of pH_{PZC} was made by plotting the ΔpH (final pH – initial pH) versus initial pH. Fourier transform infrared spectroscopy (FTIR) technique was employed to predict the functional groups present on the surface of CASB and how they interact with IBP during biosorption. The samples of CASB were prepared using the KBr disk method, and the transmission FTIR spectra were recorded in the 400 and 4000 cm^{-1} (Shimadzu IRAffinity-1 spectrophotometer). Thermogravimetric analysis (TGA) and differential thermal analysis (DTA) were carried out to evaluate the thermal stability of CASB. A Shimadzu DTG-60H thermogravimetric analyzer was used for this purpose. The analysis was conducted in an air atmosphere at a heating speed of 20 °C/min from ambient temperature (26 °C) up to 1000 °C.

2.4 Batch biosorption experiments

The experiments were conducted with 100 mL Erlenmeyer flasks containing 30 mL of the aqueous solution of IBP. Flasks were agitated on a rotary shaker at 150 rpm. The effects of different physicochemical variables on the biosorption efficiency such as pH (2, 4, 6, 8, and 10, adjusted by the addition of 0.1 M HCl or 0.1 M NaOH solutions), initial IBP concentration (5.0–25.0 mg L^{-1}), and temperature (20, 30, and 40 °C), were evaluated. After tests, the biosorbent particles were removed by filtration (filter membrane \varnothing 0.45 μm), and the residual IBP in the solution was quantified by UV–Vis spectrophotometer (Hach DR6000) at $\lambda_{\text{max}} = 221$ nm. All biosorption experiments were conducted in triplicate. IBP removal efficiency, R (%), and biosorption capacity (q_e , mg g^{-1}) of biosorbent at the equilibrium were calculated according to Equations (1) and (2), respectively.

$$R(\%) = \frac{C_i - C_e}{C_i} \times 100 \quad (1)$$

$$q_e = \frac{(C_i - C_e) \cdot B}{B} \quad (2)$$

where C_i and C_e are the initial and the equilibrium IBP concentrations (mg L^{-1}), and B is the biosorbent concentration in solution (g L^{-1}).

3. RESULTS AND DISCUSSION

3.1 FTIR, TGA/DTA analysis, and pH_{pzc}

FTIR spectra of SB, CASB, and CASB-IBP (CASB after ibuprofen biosorption) are shown in Fig. 2. The SB spectrum showed broadband in the region 3800–3000 cm^{-1} , which can be attributed to O–H stretching vibration. The band observed at 2916 cm^{-1} is assigned to the aliphatic C–H group. The peak at 1728 cm^{-1} is characteristic of the carbonyl group (C=O), present in hemicellulose. The peaks at 1604 and 1512 cm^{-1} are related to the aromatic skeletal vibrations in lignin [35]. The peaks at 1373 and 1257 cm^{-1} are assigned to C–H and C–O stretching vibrations, respectively, from the acetyl group in hemicelluloses [36]. The absorption at 1165 cm^{-1} is in connection with the asymmetric vibration of C–O–C group of the cellulose and hemicellulose [33]. The peak at 1041 cm^{-1} is attributed to C–O stretching vibration in cellulose, hemicelluloses, and lignin [36]. After chemical activation, with extraction of some compounds from SB by solvents, the peaks at 1728 (C=O) and 1604 (C=C) shifted to 1735 and 1643 cm^{-1} , respectively. Alterations in the band of hydroxyl groups (O–H stretching vibration) at region 3800–3000 cm^{-1} and in the peak of the aliphatic C–H group (2900 cm^{-1}) were also detected. After IBP biosorption, the band intensity at 3800–3000 cm^{-1} decreased, the peak at 1604 cm^{-1} shifted to 1597 cm^{-1} , and the peak at 1643 cm^{-1} disappeared. These results indicated that O–H and C=C (π - π stacking interactions between aromatic rings of the IBP and lignin) contributed to IBP adsorption on CASB.

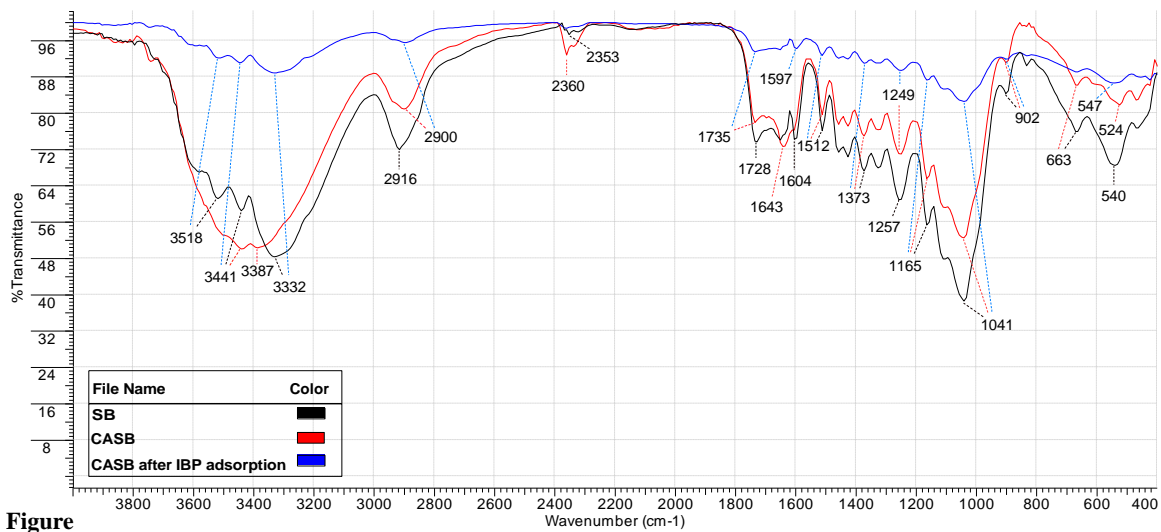


Figure 2: FTIR spectra of SB, CASB, and CASB-IBP (after ibuprofen biosorption).

The thermal behavior of the CASB is shown in Fig. 3. It is observed that the mass loss of CASB could be divided into some steps. The first step was extended from 26 to 230 °C and is due to loss of moisture and light volatile matter [37]. The second mass loss step (50.22%) was from 230 to 340 °C and corresponded to the thermal degradation of hemicellulose and cellulose [38]. This step was accompanied by an exothermic peak in the DTA curve. The third step was from 340 to 525 °C, with a mass loss of 18.33%. This step was also exothermic according to the DTA curve and is related to the thermal degradation of lignin [38]. The mass loss at the temperature range of 525-1000 °C may correspond to ashes. At 1000 °C, the total mass loss reached 74.62%.

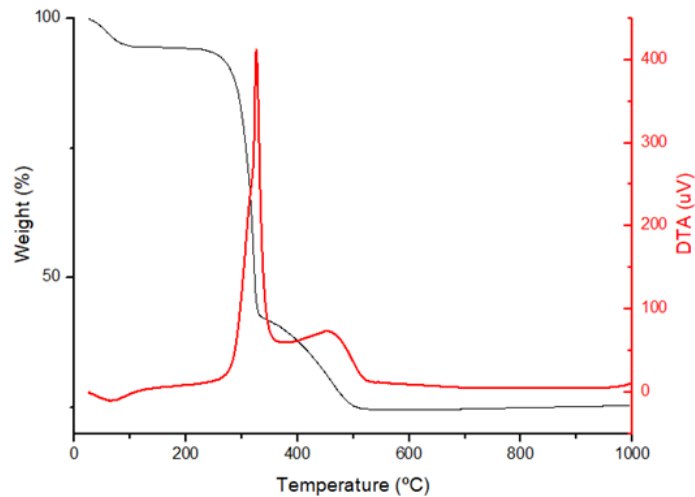


Figure 3: TGA/DTA curve of CASB.

The pH value where the net charge on the adsorbent surface is zero is the point of zero charge (pH_{pzc}). The adsorbent surface will be negatively charged when the $pH_{pzc} < pH$ of the solution, and will be positively charged when the $pH_{pzc} > pH$ of the solution. Fig. 4a shows the plot of ΔpH versus initial pH, indicating that the pH_{pzc} for CASB was found to be 7.12.

3.2 Effect of pH

The pH of the solution is crucial in the biosorption process since it influences the surface charge of the adsorbent and the solubility of adsorbates. Fig. 4b shows the effect of different initial pH on the IBP removal by CASB at 30 °C during 60 min, and 10.0 mg L⁻¹ initial IBP concentration. From these results, it was found

that IBP biosorption decreased from 3.0 to 1.1 mg g⁻¹ when the pH increased from 2.0 to 10.0. The removal of IBP by raw SB was also studied, and the results were practically negligible (<1.0 mg g⁻¹) (data not shown). The pH effect on the biosorption of IBP can be explained by the pKa value of ibuprofen and the surface charge of CASB (pH_{pzc}). The pKa value of IBP is 4.9 [39]. Above this value, the anionic form of IBP is the predominant species, while below this value, it is principally found in its molecular form [30]. Increasing the pH increases the anionic form of IBP while the CASB surface becomes less positive, which led to lesser biosorption. At pH 2, the increased IBP removal suggests an interaction between CASB surfaces with IBP by attractive H-bonds and other interactions. At the same time, electrostatic repulsion seems to be minor at this pH solution.

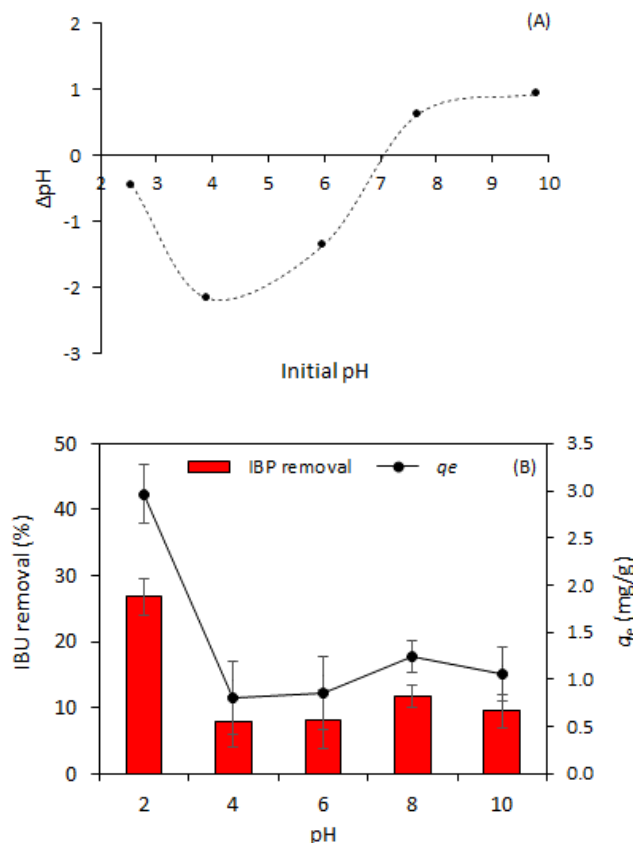


Figure 4: (A) Point of zero charge (pH_{pzc}) of CASB; (B) Effect of pH on the IBP removal by CASB (biosorbent dosage = 1.0 g L⁻¹, [IBP] = 10 mg L⁻¹, contact time = 60 min, temperature = 30 °C).

3.3 Effect of contact time and temperature

The ideal adsorbent should quickly remove the adsorbate from the liquid phase and establish the equilibrium. Fig. 5 shows the IBP biosorption by CASB at different contact times and temperatures. Rapid adsorption of IBP occurred during the first 10 min for three temperatures and was gradually slowed down until 90 min. The rapid biosorption of the IBP in the initial minutes is attributed to the high number of free active sites on the CASB surface. Also, it can be seen that the biosorption capacity of CASB decreased from 4.5 to 3.0 mg g⁻¹ when the temperature was increased from 20 to 40 °C, indicating that an exothermic process controls the biosorption of IBP onto CASB.

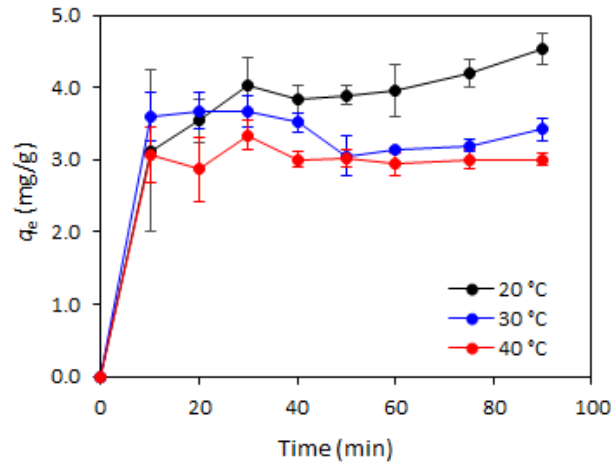


Figure 5: Effect of contact time on the IBP removal by CASB (pH = 2.0, [IBP] = 10 mg L⁻¹, biosorbent dosage = 1.0 g L⁻¹).

3.4 Biosorption kinetic

Biosorption is a time-dependent process. Thus, kinetic studies must be developed for the design and evaluation of sorbents. In this study, kinetic studies of IBP removal were conducted at constant initial IBP concentration (10.0 mg L⁻¹), 1.0 g L⁻¹ biosorbent concentration, and temperatures of 20, 30, and 40°C. Two well established kinetic models, the pseudo-first-order model [40] and pseudo-second-order model [41], were applied to investigate the biosorption of IBP on CASB.

The linearized forms of the pseudo-first-order model and pseudo-second-order model are given in Eqs. (3) and (4), respectively:

$$\log(q_e - q_t) = \log q_e - \frac{K_1}{2.303} t \quad (3)$$

$$\frac{t}{q_t} = \frac{1}{K_2 q_e^2} + \frac{1}{q_e} t \quad (4)$$

where q_e and q_t are the amounts of IBP adsorbed by biosorbent (mg g⁻¹) at equilibrium and at time t , respectively. K_1 is the pseudo-first-order rate constant (1 min⁻¹), and K_2 is the pseudo-second-order rate constant (g mg⁻¹ min⁻¹).

Table 1 shows the estimated kinetic parameters and linear correlation coefficients (R^2) from the pseudo-first-order and pseudo-second-order models. The low R^2 values ($R^2 < 0.738$) and the difference between experimental q_e and predicted q_t indicated that the pseudo-first-order model was not well suited to describe the biosorption of IBP onto CASB. On the other hand, the pseudo-second-order model showed excellent linearity with high correlation coefficients ($R^2 = 0.989-0.998$, Fig. 6) for all tested temperatures and the biosorption capacities (q_e) estimated by the models were close to those acquired by the experiments. Thus, these results suggest that the pseudo-second-order model provided a good correlation for the biosorption of IBP onto CASB in contrast to the pseudo-first-order model.

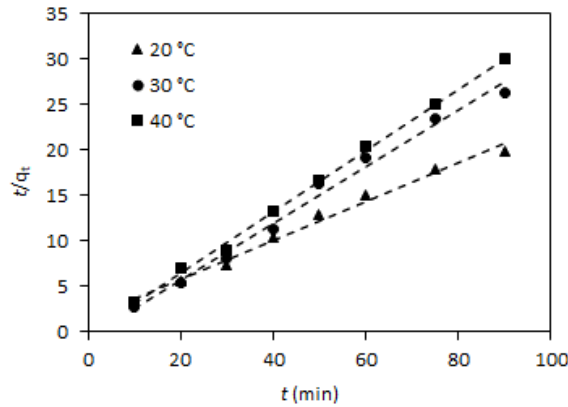


Figure 6: Plot for pseudo-second-order model for the biosorption IBP onto CASB, at different temperatures.

Table 1: Pseudo-first-order and pseudo-second-order kinetic parameters for the biosorption of IBP onto CASB, at different temperatures.

Model	Temperature (°C)		
	20	30	40
$q_{\text{experimental}}$	4.54	3.42	3.00
Pseudo-first-order			
q_1 (mg g ⁻¹)	1.37	1.28	1.45
k_1 (min ⁻¹)	1.75×10^{-2}	8.52×10^{-3}	9.21×10^{-3}
R^2	0.738	0.687	0.039
Pseudo-second-order			
q_2 (mg g ⁻¹)	4.65	3.21	2.97
k_2 (g mg ⁻¹ min ⁻¹)	3.18×10^{-2}	2.15×10^{-1}	5.43×10^{-1}
R^2	0.989	0.990	0.998

3.5 Equilibrium isotherms

Adsorption isotherms describe how adsorbates interact with adsorbents and could be used to design the sorption systems. The equilibrium experiments were carried out with different initial IBP concentrations (5-25 mg L⁻¹), using 1.0 g L⁻¹ biosorbent concentration at 20 °C. The Langmuir [42], Freundlich [43], and Dubinin-Radushkevich (D-R) [44] isotherms models were used to analyze the experimental equilibrium data of IBP biosorption. The models are represented as follows:

Langmuir isotherm:

$$\frac{1}{q_e} = \frac{1}{q_{\text{max}}} + \left(\frac{1}{q_{\text{max}}K_L} \right) \frac{1}{C_e} \quad (5)$$

Freundlich isotherm:

$$\ln q_e = \ln K_f + \frac{1}{n} \ln C_e \quad (6)$$

where q_e (mg g⁻¹) is the amount of IBP adsorbed by the biosorbent at the equilibrium, C_e (mg L⁻¹) is the IBP concentration in the solution at the equilibrium, q_{max} (mg g⁻¹) is the maximum adsorption capacity of biosorbent, K_L (L mg⁻¹) is the Langmuir constant, K_f ((mg g⁻¹)(mg L⁻¹)^{-1/n}) is the Freundlich constant, and n (di-

dimensionless) is the intensity of adsorption. The parameters of the Langmuir (q_{max} , K_L) and Freundlich (K_f , n) isotherms were calculated by plotting $1/q_e$ versus $1/C_e$ (Fig. 7a) and $\ln q_e$ versus $\ln C_e$ (Fig. 7b), respectively.

The calculated parameters for Langmuir and Freundlich isotherm models are presented in Table 2. Both models described the equilibrium data quite well, with correlation coefficients of 0.974 for the Langmuir model and 0.976 for the Freundlich model. The Langmuir isotherm model assumes monolayer adsorption onto a surface with a finite number of identical sites and negligible interaction between adsorbed molecules. The maximum monolayer adsorption capacity calculated by the Langmuir model was found to be 7.75 mg g⁻¹. Table 3 compared the maximum biosorption capacities of IBP by CASB and other biomasses. It was observed that the IBP biosorption capability using the CASB was comparable to those obtained for biomasses derived from other sources.

To determine the favorability of the biosorption, the separation factor of Langmuir isotherm (R_L) was calculated according to the Eq. (7):

$$R_L = 1/(1 + K_L C_i) \quad (7)$$

where C_i (mg L⁻¹) is the highest initial IBP concentration, K_L (L mg⁻¹) is the Langmuir constant, and R_L is a dimensionless constant which indicates whether isotherm is favorable ($0 < R_L < 1$), unfavorable ($R_L > 1$), linear ($R_L = 1$) or reversible ($R_L = 0$). In this study, the R_L value was 0.648, indicating that the sorption process is favorable.

The Freundlich isotherm model describes multilayer adsorption occurring on an energetically heterogeneous surface. The value of n is suitable to predict the type of isotherm, indicating a favorable adsorption process when $1 < n < 10$. Unexpectedly, the n value was 0.825, suggesting an unfavorable adsorption process, which was against the separation factor of Langmuir isotherm ($R_L = 0.648$) and the considerable biosorption capacity of CASB (7.75 mg g⁻¹). According to Hui *et al.* [45], the Freundlich isotherm model is frequently applied in strictly empirical cases; therefore, unfavorable adsorption conditions in practice may lead to unsatisfactory parameters.

The D-R isotherm model was used to determine the nature of the adsorption process as chemical or physical. The D-R model is expressed by Eq. (8):

$$q_e = q_m e^{-\beta \varepsilon^2}; \quad \varepsilon = RT \ln \left(1 + \frac{1}{C_e} \right) \quad (8)$$

where q_e (mol g⁻¹) is the amount of IBP adsorbed on the biosorbent, q_m (mol g⁻¹) is the maximum biosorption capacity, β (mol² kJ⁻²) is the constant related to the mean free energy of biosorption, ε is the Polanyi potential, R (8.314 J mol⁻¹ K⁻¹) is the ideal gas constant, and T (K) is the absolute temperature. From the activity coefficient β , it is possible to estimate the mean free energy of biosorption (E , kJ mol⁻¹), according to Equation (9):

$$E = \frac{1}{\sqrt{2\beta}} \quad (9)$$

When E value falls in the range from 8 to 16 kJ mol⁻¹, the biosorption process is controlled by a chemical mechanism. For $E < 8$ kJ mol⁻¹, the biosorption process proceeds through a physical mechanism. As shown in Table 2, the E value of 7.07 kJ mol⁻¹ indicated that IBP was adsorbed onto CASB following a physical process.

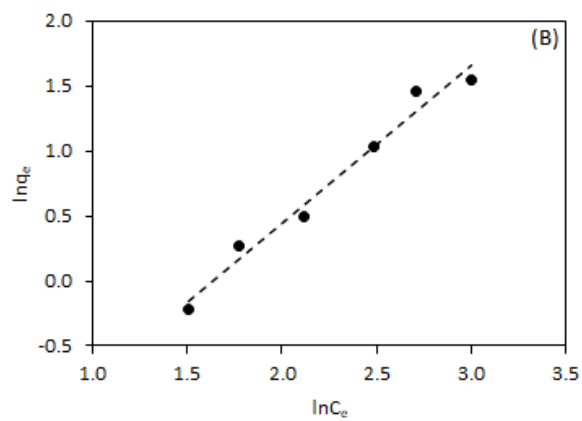
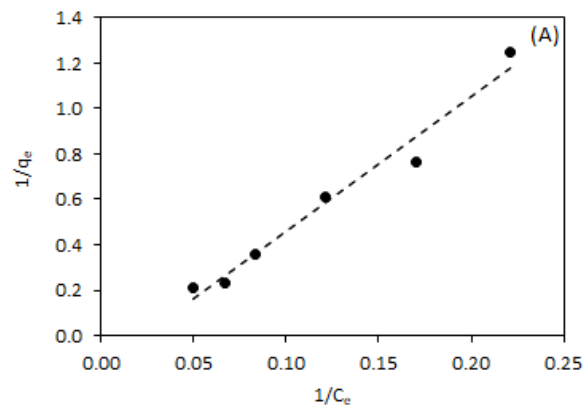
Table 2: Isotherm parameters for the biosorption of IBP onto CASB.

Model	Parameter
Langmuir	
q_{max} (mg g ⁻¹)	7.75
K_L (L mg ⁻¹)	2.19 x 10 ⁻²
R^2	0.974
Freundlich	
K_F (mg g ⁻¹) (mg L ⁻¹) ^{-1/n}	0.138

n	0.825
R^2	0.976
D-R	
q_m (mmol g ⁻¹)	4.257
β (mol ² J ⁻²)	1.00 x 10 ⁻⁸
E (kJ mol ⁻¹)	7.07
R^2	0.978

Table 3: Maximum biosorption capacity of IBP onto CASB and other biosorbents.

Adsorbent	q_{max} (mg/g)	Reference
Biomass of the microalga <i>Phaeodactylum tricornutum</i>	3.97	[46]
<i>Parthenium hysterophorus</i> biochar	3.759	[30]
Wood apple biochar	5.00	[47]
Chemically activated sugarcane bagasse (CASB)	7.75	Present study
Pine wood biochar	10.74	[48]
Sugarcane bagasse physically activated biochar	11.90	[32]
Wood apple steam activated biochar	12.66	[47]



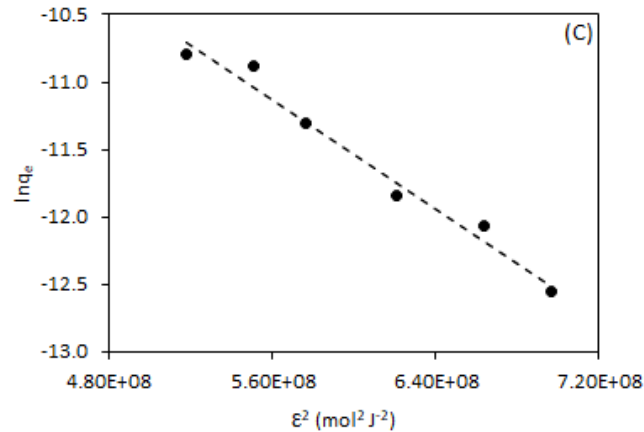


Figure 7. Linearized plots of the isotherm models: (a) Langmuir, (b) Freundlich, and (c) Dubinin- Radushkevich (D-R).

3.6 Thermodynamic parameters

The thermodynamics parameters of IBP biosorption onto CASB, *i.e.*, Gibbs free energy change (ΔG), entropy (ΔS), and enthalpy (ΔH) were calculated by using the Equations (10) through (12):

$$\Delta G = -RT \ln K_D \quad (10)$$

$$(11)$$

$$\Delta G = \Delta H - T\Delta S$$

$$(12)$$

$$\ln K_D = \frac{\Delta S}{R} - \frac{\Delta H}{R} \times \frac{1}{T}$$

where R is the universal gas constant (8.314 J/K mol), K_D (qe/Ce) is the distribution coefficient, and T (K) is the absolute temperature. Values of ΔS and ΔH were calculated from the Van't Hoff plot of $\ln K_D$ versus $1/T$ (Fig. 8).

Table 4 summarizes the thermodynamic parameters calculated at different temperatures (20, 30, and 40 °C). The negative ΔH value of -23.64 KJ mol⁻¹ suggests an exothermic biosorption process that is facilitated with a decrease in temperature. The ΔS was also found to be negative (-84.007 J mol⁻¹ K⁻¹), revealing that the randomness at the solid/solution interface decreases during the biosorption of the IBP. The positive values of ΔG indicate the presence of an energy barrier in the IBP biosorption onto CASB.

Table 4. Thermodynamic parameters estimated for IBP biosorption onto CASB.

T (°C)	K_D	ΔG (KJ mol ⁻¹)	ΔH (KJ mol ⁻¹)	ΔS (J mol ⁻¹ K ⁻¹)
20	0.70	0.981	-23.64	-84.0
30	0.44	1.821		
40	0.38	2.661		

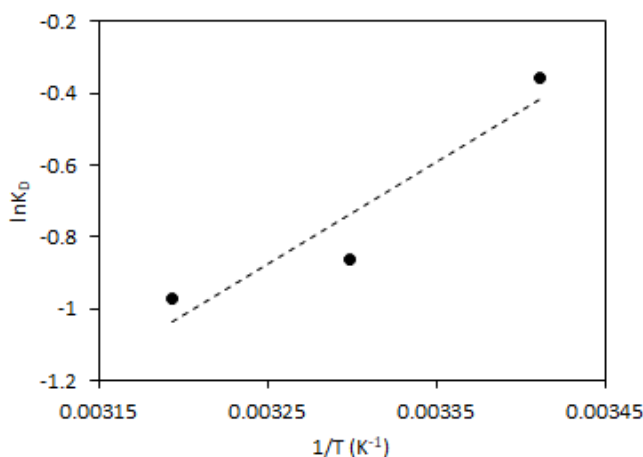


Figure 8. Plot of $\ln K_D$ versus $1/T$ for estimation of thermodynamic parameters.

4. CONCLUSIONS

The present study revealed that sugarcane bagasse activated by hexane and methanol could be used as a biosorbent to remove IBP from aqueous solution. Higher biosorption rates were obtained at pH 2.0. Pseudo-second-order kinetic model was found to explain the biosorption data most effectively. The equilibrium study showed that both Langmuir and Freundlich isotherm models described the experimental data with accuracy. The maximum biosorption capacity was estimated at 7.75 mg g^{-1} at 20°C . The IBP biosorption onto CASB was physical, exothermic and, non-spontaneous.

5. ACKNOWLEDGMENTS

This study was financed in part by the Coordenação de Aperfeiçoamento de Pessoal de Nível Superior – Brasil (CAPES) – Finance Code 001

6. BIBLIOGRAPHY

- [1] COUTO, C. F., LANGE, L. C., AMARAL, M. C. S. "Occurrence, fate and removal of pharmaceutically active compounds (PhACs) in water and wastewater treatment plants — A review", *J. Water Process. Eng.*, v. 32, pp. 1-17, 2019.
- [2] AHKOLA, H., TUOMINEN, S., KARLSSON, S., *et al.*, "Presence of active pharmaceutical ingredients in the continuum of surface and ground water used in drinking water production", *Environ. Sci. Pollut. Res.*, v. 24, pp. 26778-26791, 2017.
- [3] THIEBAULT, T., CHASSIOT, L., FOUGÈRE, L., *et al.*, "Record of pharmaceutical products in river sediments : A powerful tool to assess the environmental impact of urban management?", *Anthropocene*, v. 18, pp. 47-56, 2017.
- [4] ARISTIZABAL-CIRO, C., BOTERO-COY, A. M., LÓPEZ, F. J., *et al.*, "Monitoring pharmaceuticals and personal care products in reservoir water used for drinking water supply", *Environ. Sci. Pollut. Res.* v. 24, pp. 7335-7347, 2017..
- [5] TRÖGER, R., KLÖCKNER, P., AHRENS, L., *et al.*, "Micropollutants in drinking water from source to tap - Method development and application of a multiresidue screening method". *Sci. Total Environ.* v. 627, pp. 1404-1432, 2018.
- [6] MARCHLEWICZ, A, GUZIK, U., HUPERT-KOCUREK, K. Toxicity and biodegradation of ibuprofen by *Bacillus* 2017;1:7572–84. <https://doi.org/10.1007/s11356-017-8372-3>.
- [7] FERREIRA, R. C., LIMA, H.H.C., *et al.*, "Utilização de carvão ativado de dendê in natura e funcionalizado em meio ácido na adsorção de paracetamol". *Rev. Mater.* v. 23, pp. 1-11, 2018.
- [8] OLIVEIRA, M., FRIHLING, B.E.F., VELASQUES, J., *et al.*, "Pharmaceuticals residues and xenobiotics contaminants: Occurrence, analytical techniques and sustainable alternatives for wastewater treatment", *Sci. Total Environ.*, v. 705, pp. 1-16, 2020.
- [9] KOT-WASIK, A., JAKIMSKA, A., ŚLIWKA-KASZYŃSKA, M. "Occurrence and seasonal variations of 25 pharmaceutical residues in wastewater and drinking water treatment plants", *Environ. Monit. Assess.*, v. 188, pp. 1-13, 2016.
- [10] RAGUGNETTI, M., ADAMS, M. L., GUIMARÃES, A. T. B. "Ibuprofen genotoxicity in aquatic environment: an experimental model using *Oreochromis niloticus*", *Water Air Soil Pollut.*, v. 218, pp. 361-364, 2011.

- [11] CASTELL, J. V., GOMEZ-L, M. J., MIRANDA, M. A., *et al.*, "Photolytic degradation of ibuprofen. Toxicity of the isolated photoproducts on fibroblasts and erythrocytes", *Photochem. Photobiol.* v. 46, pp. 991–996, 1987.
- [12] HUNG, C. H., YUAN, C., WU, M. H., *et al.*, "Electrochemical degradation of ibuprofen-contaminated soils over Fe/Al oxidation electrodes", *Sci. Total Environ.* v. 640–641, pp. 1205–1213, 2018.
- [13] HUSSAIN, S., ANEGGI, E., BRIGUGLIO, S., *et al.*, "Enhanced ibuprofen removal by heterogeneous-Fenton process over Cu/ZrO₂ and Fe/ZrO₂ catalysts", *J. Environ. Chem. Eng.* v. 8, pp. 1-9, 2020.
- [14] JIMÉNEZ-SALCEDO, M., MONGE, M., TENA, M. T. "Photocatalytic degradation of ibuprofen in water using TiO₂/UV and g-C₃N₄/visible light: Study of intermediate degradation products by liquid chromatography coupled to high-resolution mass spectrometry", *Chemosphere*, v. 215, pp. 605-618, 2019.
- [15] AL-HAMADANI, Y. A. J., PARK, C. M., ASSI, L. N., *et al.*, "Sonocatalytic removal of ibuprofen and sulfamethoxazole in the presence of different fly ash sources", *Ultrason Sonochem.*, v. 39, pp. 354-362, 2017.
- [16] JOTHINATHAN, L., HU, J. "Kinetic evaluation of graphene oxide based heterogenous catalytic ozonation for the removal of ibuprofen", *Water Res.*, v. 134, pp. 63-73, 2018.
- [17] ZHANG, L., LV, T., ZHANG, Y. *et al.*, "Effects of constructed wetland design on ibuprofen removal – A mesocosm scale study", *Sci. Total Environ.*, v. 609, pp. 38-45, 2017.
- [18] SANTOS, B. A. P., COSSOLIN, A. S., REIS, H. C. O., *et al.*, "Baker's yeast-MnO₂ composites as biosorbent for Malachite green: An ecofriendly approach for dye removal from aqueous solution", *Rev. Ambient. e Água*, v. 14, pp. 1-15, 2019.
- [19] DE ROSSI, A., RIGUETO, C. V. T., DETTMER, A., *et al.*, "Synthesis, characterization, and application of *Saccharomyces cerevisiae*/alginate composites beads for adsorption of heavy metals", *J. Environ. Chem. Eng.*, v. 8, pp. 1-7, 2020.
- [20] BELLO, O. S., ALAO, O. C., ALAGBADA, T. C., *et al.*, "Biosorption of ibuprofen using functionalized bean husks", *Sustain. Chem. Pharm.*, v. 13, pp. 1-10, 2019.
- [21] CASTRO, K. C., COSSOLIN, A. S., REIS, H. C. O., *et al.*, "Biosorption of anionic textile dyes from aqueous solution by yeast slurry from brewery", *Braz. Arch. Biol. Technol.*, v.60, pp.1-13, 2017.
- [22] XAVIER, C. S. F., CRISPINIANO, F. F., NASCIMENTO, K. K. R., *et al.*, "Secagem e avaliação do bagaço de cana de açúcar como adsorvente de corantes têxteis presentes em soluções aquosas". *Rev. Mater.* v. 26, pp. 1-13, 2021.
- [23] LEANDRO-SILVA, E., PIPI, A. R. F., MAGDALENA, A. G., *et al.*, "Application of Langmuir and Freundlich models in the study of banana peel as bioadsorbent of copper (II) in aqueous medium". *Rev. Mater.* v. 25, pp. 1-12, 2020.
- [24] MONDAL, S., BOBDE, K., AIKAT, K., *et al.*, "Biosorptive uptake of ibuprofen by steam activated biochar derived from mung bean husk: Equilibrium, kinetics, thermodynamics, modeling and eco-toxicological studies", *J. Environ. Manage.*, v. 182, pp. 581-594, 2016.
- [25] ABBAS, G., HAIDER, R., HUSSAIN, F. "Adsorption of non-steroidal anti-inflammatory drugs (Diclofenac and ibuprofen) from aqueous medium onto activated onion skin", *Desalin. Water Treat.*, v. 95, pp. 274-285, 2017.
- [26] PEÑAFIEL, M. E., MATESANZ, J. M., VANEGAS, E., *et al.*, "Corncobs as a potentially low-cost biosorbent for sulfamethoxazole removal from aqueous solution", *Sep. Sci. Technol.*, pp. 1-12, 2019.
- [27] KHADIR, A., NEGARESTANI, M., MOLLAHOSSEINI, A. "Sequestration of a non-steroidal anti-inflammatory drug from aquatic media by lignocellulosic material (*Luffa cylindrica*) reinforced with polypyrrole: Study of parameters, kinetics, and equilibrium", *J. Environ. Chem. Eng.*, v. 8, pp. 1-14 2020.
- [28] CARVALHO, R. S., ARGUELHO, M. L. P. M., FACCIOLI, G. G., *et al.*, "Use of orange bagasse biocarbon for the removal of tetracycline in wastewater". *Rev. Mater.* v. 26, pp. 1-14, 2021.
- [29] KAIS, H., YEDDOU MEZENNER, N., TRARI, M. "Biosorption of rifampicin from wastewater using cocoa shells product", *Sep. Sci. Technol.*, pp. 1-10, 2019.
- [30] MONDAL, S., AIKAT, K., HALDER, G. "Biosorptive uptake of ibuprofen by chemically modified *Parthenium hysterophorus* derived biochar: Equilibrium, kinetics, thermodynamics and modeling", *Ecol. Eng.*, v. 92, pp. 158-172, 2016.
- [31] ABBAS, G., JAVED, I., IQBAL, M. *et al.*, "Adsorption of non-steroidal anti-inflammatory drugs (Diclofenac and ibuprofen) from aqueous medium onto activated onion skin. *Desalin. Water Treat.*, v. 95, pp. 274-285, 2017.
- [32] CHAKRABORTY, P., SHOW, S., BANERJEE, S., *et al.*, "Mechanistic insight into sorptive elimination of ibuprofen employing bi-directional activated biochar from sugarcane bagasse: Performance evaluation and cost estimation" *J. Environ. Chem. Eng.*, v. 6, pp. 5287–5300, 2018.
- [33] MOTHÉ, C. G., MIRANDA, I. C. "Characterization of sugarcane and coconut fibers by thermal analysis and FTIR", *J. Therm. Anal. Calorim.* v. 97, pp. 661–665, 2009.
- [34] DAHRI, M. K., KOOH, M. R. R., LIM, L. B. L. "Water remediation using low cost adsorbent walnut shell for removal of malachite green: Equilibrium, kinetics, thermodynamic and regeneration studies", *J. Environ. Chem. Eng.*, v. 2, pp. 1434–1444, 2014.
- [35] TAJERNIA, H., EBADI, T., NASERNEJAD, B. "Arsenic removal from water by sugarcane bagasse: an application of response surface methodology (RSM)", *Water Air Soil Pollut.*, v. 225, pp. 1-22, 2014.

- [36] YU, J., WANG, L., CHI, R. *et al.*, "Adsorption of Pb²⁺, Cd²⁺, Cu²⁺, and Zn²⁺ from aqueous solution by modified sugarcane bagasse", *Res. Chem. Intermed.*, v. 41, pp. 1525–1541, 2015.
- [37] ATTIA, L. A., YOUSSEF, M. A., MOAMEN, O. A. A. "Feasibility of radioactive cesium and europium sorption using valorized punica granatum peel : kinetic and equilibrium aspects", *Sep. Sci. Technol.* pp. 1-16, 2019.
- [38] VARMA, A. K., MONDAL, P. "Physicochemical characterization and pyrolysis kinetic study of sugarcane bagasse using thermogravimetric analysis", *J. Energy Resour. Technol.*, v. 138, pp. 1–11, 2016.
- [39] LINDQVIST, N., TUHKANEN, T., KRONBERG, L. "Occurrence of acidic pharmaceuticals in raw and treated sewages and in receiving waters", *Water Res.*, v. 39, pp. 2219–2228, 2005.
- [40] LAGERGREN, S. Y. "Zur theorie der sogenannten adsorption gelöster stoffe, kungliga svenska vetenskapsakademiens", *Handlingar*, v. 24, pp. 1–39, 1898.
- [41] HO, Y., MCKAY, G. "Pseudo-second order model for sorption processes", *Process. Biochem.*, v. 34, pp. 451-465, 1999.
- [42] LANGMUIR, I. "The adsorption of gases on plane surfaces of glass, mica and platinum", *J. Am. Chem. Soc.*, v. 40, pp. 1361-1402, 1918.
- [43] FREUNDLICH, H. "Über die Adsorption in Lösungen", *Zeitschrift Für Phys. Chemie*, v. 57, pp. 385-470, 1906.
- [44] DUBININ, M. M., RADUSHKEVICH, L. V. "Equation of the characteristic curve of activated charcoal", *Proc. Acad. Sci. USSR*, v. 55, pp. 331–333, 1947.
- [45] HUI, C., GUO, X., SUN, P., *et al.*, "Bioresource Technology Removal of nitrite from aqueous solution by *Bacillus amyloliquefaciens* biofilm adsorption", *Bioresour. Technol.*, v. 248, pp. 146–152, 2018.
- [46] SANTAUFEMIA, S., TORRES, E., ABALDE, J. "Biosorption of ibuprofen from aqueous solution using living and dead biomass of the microalga *Phaeodactylum tricorutum*", *J. Appl. Phycol.*, v. 30, pp. 471–482, 2018.
- [47] CHAKRABORTY, P., BANERJEE, S., KUMAR, S., *et al.*, "Elucidation of ibuprofen uptake capability of raw and steam activated biochar of *Aegle marmelos* shell: Isotherm, kinetics, thermodynamics and cost estimation", *Process Saf. Environ. Prot.*, v. 118, pp. 10–23, 2018.
- [48] ESSANDOH, M., KUNWAR, B., PITTMAN, C.U., *et al.*, "Sorbptive removal of salicylic acid and ibuprofen from aqueous solutions using pine wood fast pyrolysis biochar", *Chem. Eng. J.*, v. 265, pp. 219–227, 2015.

ORCID

Bruna Assis Paim dos Santos

<https://orcid.org/0000-0003-0061-7900>

Evandro Luiz Dall'Oglio

<http://orcid.org/0000-0002-8936-5107>

Adriano Buzutti de Siqueira

<https://orcid.org/0000-0002-4632-4014>

Leonardo Gomes de Vasconcelos

<http://orcid.org/0000-0002-2886-1887>

Eduardo Beraldo de Morais

<http://orcid.org/0000-0002-8505-4133>